A Finite-Element Approach to Control the End-Point Motion of a Single-Link Flexible Robot

Eduardo Bayo
Center for Robotics Systems in Microelectronics, Department of Mechanical Engineering, University of California, Santa Barbara, California 93106
Received July 28, 1986; accepted September 11, 1986

A structural finite-element technique based on Bernoulli-Euler beam theory is presented which will permit the finding of the torques (or forces) that are necessary to apply at one end of a flexible link to produce a desired motion at the other end. This technique is suitable for the open loop control of the tip motion. It may also provide a good control law for feedback control. The finite-element method is used to discretize the equations of motion. This method has a major advantage in the fact that different material properties and boundary conditions like hubs, tip loads, changes in cross sections, etc., can be handled in a very simple and straightforward manner. The resulting differential equations are integrated via the frequency domain. This allows for the expansion of the desired end motion into its harmonic components and helps to visualize the complex wave propagation nature of the problem. The performance of the proposed technique is illustrated in the solution of a practical example. Results point out the potential that this technique has in the study of the dynamics and control not only of flexible robots, but also of any other flexible mechanisms like those used in biomechanics, where high precision at the tip of very light flexible arms is required.

ベルヌーイ・オイラーのはり理論に基づく構造工学における有限要素法を本論文は論じている。柔軟なリンクの一端において必要な動きを得るために他端に与えるべきトルク（または力）が本方式により求まる。この技法は先端の動作を開ループ制御するのに適しているし、フィードバック制御のためのよい制御規則を与えることができる。有限要素法は変位方程式を離散化する際に用いられる。こしき、先端負荷、断面の変化などの様々な材質や境界条件が、きわめて単純かつ一様に取り扱えることが本方式の特徴である。得られた微分方程式は周波数領域において積分される。このことにより、所要の先端の動きが高調波成分へ展開され、この問題の波動伝播としての複雑な特性を視覚化するのを助けている。実際の例題を解くことによって、ここに提案された方式のよさが示された。柔軟なロボットだけでなく（きわめて軽い柔軟な腕の手先において高い精度が要求されるような）バイオメカニクスにおいて使用されるような様々なメカニズムの動特性と制御の研究におけるこの方式の可能性を、この結果は示している。

Journal of Robotic Systems, 4(1), 63–75 (1987)
 CCC 0471-2223/87/010063-13$04.00

INTRODUCTION

A new generation of faster and more precise robots, like those in use in the microelectronic industry, is emerging. More and more demand is being placed on robots with higher speeds, smaller actuators, larger members, and higher payload capacity. Due to the flexible oscillations, the assumption of rigid dynamics and kinematics is no longer applicable and the study of these robots considering the flexibility of the links becomes necessary. Tools for the modeling and analysis of flexible links have been presented among others by Sunada,[1] Chang,[2] Geradin *et al.*,[3] and more recently by Naganathan and Soni.[4]

On the other hand, the oscillatory behavior of the flexible links makes it difficult to control the end-point motions for a desired accuracy within an adequate time interval. The central problem lies in the control of the end-point motion by applying the proper torques at the actuating points. The interaction between the links' elasticity and the control system further complicates the problem, particularly at high speeds. A technique for end-control motion corroborated by experimental work has been introduced by Cannon and Schmitz.[5] They proposed a series of stable control strategies for a single-link flexible manipulator with sensors and actuators situated at opposite ends. A similar approach based on a more involved analytical model of the link and different sensor system has been presented by Sakawa *et al.*[6] Another method for the suppression of vibrational motion by using modal space control has been presented by Karkkainen.[7] The idea of supplementing torque control at the joints by application of force pulses at specific points along the links was proposed by Chassiakos and Bekey.[8] Lumped parameter nonlinear continuous models of flexible articulated one-link and two-link robots, along with control algorithms have been suggested by Nicosia *et al.*[9]

The method proposed herein aims at controlling the tip motion by directly computing the torque necessary to apply at one end of the link to achieve the desired motion at the other end, taking into consideration the flexibility of the link. A variational approach and the finite element method are used to discretize the equations of motion. The main advantage of this method lies in the flexible and natural manner in which boundary conditions and physical properties may be imposed. In particular, conditions commonly present in robots, such as tip payloads, pointwise inertias like hubs, or changes in geometric properties and cross sections, may be modeled in a very straightforward way.

Using the finite-element method the partial differential equations of motion are transformed into a set of second-order differential equations in terms of the displacement, velocities and accelerations of the finite-element coordinates, and the unknown forcing function at the end of the link. The solution for the unknown torque requires, in the time domain, a solution of a set of Volterra-type integrodifferential equations. In this case the frequency domain provides a simpler way of solving the equations, since they can be transformed via the fast Fourier transform in a symmetric set of complex simultaneous equations.

In what follows is the formulation of the problem first described. Hamilton's principle provides the variational method upon which the finite-element weak form is built. For the beam theory the Euler-Bernoulli model is used. Rotary inertia and shear deformation are thus neglected. The discretized equations of motions are expressed in terms of

absolute or total displacements. An efficient numerical algorithm is then proposed for the solution of the equations.

Finally, the proposed technique is applied to a particular flexible one-link robot. Results illustrate the potential this technique has for the control of tip motions of flexible mechanisms.

FORMULATION OF THE PROBLEM

Consider the flexible link of constant section depicted in Figure 1 that has a total length equal to L, a hub at one end of inertia I_H, mass per unit length $\overline{m}$, Young's modulus E, and constant moment of inertia I. Let us call the total displacement at a particular location and time $v(x,t)$. This displacement is given by the hub angle $\theta(t)$ and the deflection $w(x,t)$ measured from the line x axis so that

$$v(x,t) = w(x,t) + x\,\theta(t). \tag{1}$$

Assuming Bernoulli-Euler beam theory and small elastic displacements, and neglecting the internal damping forces (they will be included later on in the formulation), the total kinetic and potential energy may be expressed in terms of $v(x,t)$ as follows:

$$U = \tfrac{1}{2}\int_0^L \overline{m}[\dot{v}(x,t)]^2\,dx + \tfrac{1}{2} I_H\,\dot{\theta}^2(t) \tag{2}$$

and

$$V = \tfrac{1}{2}\int_0^L EI[v_{,xx}(x,t)]^2\,\mathrm{dx}. \tag{3}$$

A dot and subscript x denote partial derivative with respect to time and space, respectively. The work done by the nonconservative actuating torque is equal to

$$W = T(t)\,\theta(t) \tag{4}$$

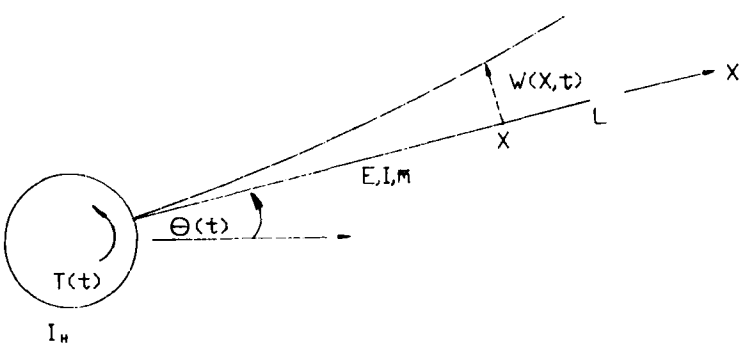

Figure 1. Deformation in a flexible arm.

The application of Hamilton's principle yields

$$\int_{t1}^{t2} \delta(U - V)\, dt + \int_{t1}^{t2} \delta W\, dt = 0. \tag{5}$$

The substitution of Eqs. (2)–(4) in (5) renders

$$\int_{t1}^{t2} \left[\int_{o}^{L} (m\dot{v}(x,t)\, \delta\dot{v} - EI\, v_{,xx}(x,t)\, \delta v_{,xx})\, dx + \right.$$
$$\left. + I_H\, \dot{\theta}\, \delta\dot{\theta} + T\delta\theta \right] = 0. \tag{6}$$

After integrating the velocity terms by parts (6) becomes

$$\int_{t1}^{t2} \left[\int_{o}^{L} (m\ddot{v}(x,t)\, \delta v + EI\, v_{,xx}\,(x,t)\, \delta v_{,xx})\, dx + \right.$$
$$\left. + I_H\, \ddot{\theta}(t)\, \delta\theta - T\delta\theta \right] = 0. \tag{7}$$

At this point the displacement field can be discretized using a finite element expansion:

$$v(x,t) = \sum_{i=1}^{N} Ni(x)\, v_i(t), \tag{8}$$

where $Ni(x)$ are the Hermite polynonials that satisfy the conditions for admissability and that are defined over the fraction of the length that constitutes the finite element. $v_i(t)$ represents the variation of the nodal displacements with time, and N is the total number of degrees of freedom. The accelerations and curvatures may now be expressed as follows:

$$\ddot{v}(x,t) = \sum_{i=1}^{N} Ni(x)\, \ddot{v}_i(t) \tag{9}$$

and

$$v_{,xx}\,(x,t) = \sum_{i=1}^{N} Ni_{,xx}\,(x)\, v_i(t). \tag{10}$$

Substitution of Eqs. (8)–(10) in (7) and proper integration will yield the link mass and stiffness matrices and the forcing vector. The reader is referred to any of the

numerous works that deal with the finite-element method, e.g., Bathe,[10] for a detailed explanation of the derivation of the mentioned matrices.

The assembled set of differential equations in terms of the nodal total displacements and accelerations becomes

$$\begin{bmatrix} M_{hh} & M_{hi} & 0 \\ M_{ih} & M_{ii} & M_{it} \\ 0 & M_{ti} & M_{tt} \end{bmatrix} \begin{bmatrix} \ddot{v}_h \\ \ddot{v}_i \\ \ddot{v}_t \end{bmatrix} + \begin{bmatrix} K_{hh} & K_{hi} & 0 \\ K_{ih} & K_{ii} & K_{it} \\ 0 & K_{ti} & K_{tt} \end{bmatrix} \begin{bmatrix} v_h \\ v_i \\ v_t \end{bmatrix} = \begin{bmatrix} T(t) \\ 0 \\ 0 \end{bmatrix}. \quad (11)$$

The three partitions in Eq. (11) refer, respectively, to the degree of freedom at the hub $v_h = \theta$, those between the tip and the hub (or internal degrees of freedom) v_i, and the translational degree of freedom at the tip v_t, as shown in Figure 2. The physical property matrices, mass, stiffness, and damping, are partitioned correspondingly. The internal viscous damping matrix can now be formed directly from the mass and stiffness matrices for a given damping ratio in terms of the Caughey series.[11] Equation (11) may be expressed in reduced form as follows:

$$\mathbf{M}\begin{bmatrix} \ddot{v}_h \\ \ddot{v}_i \\ \ddot{v}_t \end{bmatrix} + \mathbf{C}\begin{bmatrix} \dot{v}_h \\ \dot{v}_i \\ \dot{v}_t \end{bmatrix} + \mathbf{K}\begin{bmatrix} v_h \\ v_i \\ v_t \end{bmatrix} = \begin{bmatrix} T(t) \\ 0 \\ 0 \end{bmatrix}. \quad (12)$$

The total response of the system is usually contained in only a few modes of vibration. It may be convenient at this stage to reduce the set of Eqs. (12) by using the normal modes of the system. A modal analysis followed by a change to generalized modal coordinates with the corresponding matrix transformations will render a reduced set of uncoupled equations.

This reduction is avoided here for the sake of generality and also to maintain the formulation as clear as possible without further analytical complications. However, the modal approach to reduce the total number of degrees of freedom may become necessary if this analytical technique is to be used for control purposes. It is worth pointing out the major advantage introduced using finite elements, by which mode shapes and frequencies can readily be obtained when complicated boundary conditions

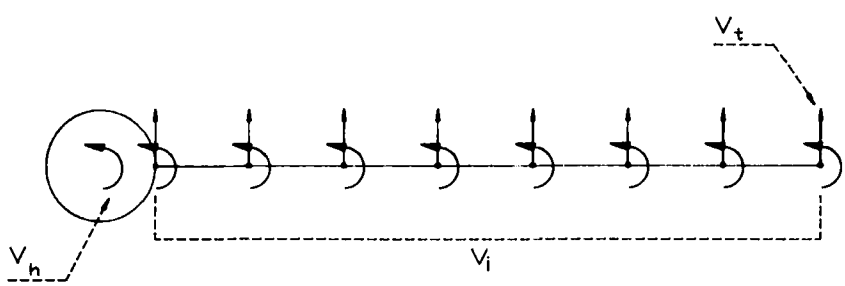

Figure 2. Finite-element degrees of freedom.

are present. The solution of the eigenvalue problem directly from the partial differential equation and boundary conditions can be very involved, particularly when the latter are complex.

We are seeking the solution for $T(t)$ in the set of differential equations (12) that produces a desired motion at the tip $v_t(t)$. In the time domain $T(t)$ could be expressed as convolution integrals between appropriate impulse responses at the tip, leading to a set of Volterra type of integrodifferential equations. It is more convenient and effective to solve for $T(t)$ by a frequency-domain analysis.

The system of equations (12) can be transformed by means of the fast Fourier transform (FFT) into independent sets of simultaneous complex equations. The number of sets is equal to the number of Fourier pairs, and the frequencies associated with each pair are equal to

$$\bar{w}_n = (2\pi/P)n, \tag{13}$$

where P is the total time over which the response is analyzed. The set of complex equations for a particular frequency $\bar{w}$ becomes

$$\left[\mathbf{M} + \frac{1}{i\bar{w}}\mathbf{C} - \frac{1}{\bar{w}^2}\mathbf{K}\right]\begin{bmatrix}\hat{\bar{v}}_h \\ \hat{\bar{v}}_i \\ \hat{\bar{v}}_t\end{bmatrix} = \begin{bmatrix}\hat{T}(\bar{w}) \\ 0 \\ 0\end{bmatrix}, \tag{14}$$

where the caret stands for the Fourier transform. In the frequency domain the damping forces may be expressed in a more convenient way by introducing the complex stiffness matrix.[12] The set of equations (14) may be thus expressed as

$$\left[\mathbf{M} - \frac{1}{\bar{w}_2}\mathbf{K}^*\right]\begin{bmatrix}\hat{\bar{v}}_h \\ \hat{\bar{v}}_i \\ \hat{\bar{v}}_t\end{bmatrix} = \begin{bmatrix}\hat{T}(\bar{w}) \\ 0 \\ 0\end{bmatrix}, \tag{15}$$

where

$$K^* = K[1 + 2i\xi], \tag{16}$$

and where ξ represents the material damping ratio. Equation (15) may be expressed in simplified notation as

$$\mathbf{H}\begin{bmatrix}\hat{\bar{v}}_h \\ \hat{\bar{v}}_i \\ \hat{\bar{v}}_t\end{bmatrix} = \begin{bmatrix}\hat{T}(\bar{w}) \\ 0 \\ 0\end{bmatrix}. \tag{17}$$

The transfer matrix $\mathbf{H}$ is a complex regular symmetric matrix except for $\bar{w} = 0$ for which it is indeterminant. However, the system does not need to be analyzed for $\bar{w} = 0$ because the zero frequency content of the desired tip acceleration is also zero.

$\hat{T}(\overline{w})$ may be obtained by solving the system of equations (17) for each of the frequencies $\overline{w}$. It is important to note that each $\overline{w}$ also represents the frequency of the harmonic waves that integrate the given motion. Those flexural waves having frequencies similar to the natural frequencies of the system will be amplified due to resonance effects, and will form the main part of the total response. The very high-frequency waves will be damped out quickly by the internal damping mechanisms. It becomes obvious then that previous knowledge of the natural frequencies of the system will help in identifying that part of the frequency spectrum in which the total response is concentrated. Equation (17) will need to be solved for only those frequencies contained in that part of the frequency spectrum.

The solution of Eq. (17) yields

$$\begin{bmatrix} \hat{\hat{v}}_h \\ \hat{\hat{v}}_i \\ \hat{\hat{v}}_t \end{bmatrix} = \begin{bmatrix} G_{hh} & G_{hi} & G_{ht} \\ G_{ih} & G_{ii} & G_{it} \\ G_{th} & G_{ti} & G_{tt} \end{bmatrix} \begin{bmatrix} T(\overline{w}) \\ 0 \\ 0 \end{bmatrix} = \mathbf{G} \begin{bmatrix} T(\overline{w}) \\ 0 \\ 0 \end{bmatrix}, \tag{18}$$

where **G** is the inverse of the transfer matrix **H.**

From (18) it is obvious that

$$\hat{\hat{v}}_t = G_{th}\, \hat{T}(\overline{w}), \tag{19}$$

and therefore

$$\hat{T}(w) = G_{th}^{-1}\, \hat{\hat{v}}_t; \tag{20}$$

therefore the torque may be computed directly from the given tip acceleration. Once $\hat{T}(\overline{w})$ is known, the angle at the hub and the internal displacements are given by

$$\begin{aligned} \hat{\hat{v}}_h &= \hat{\hat{\theta}} = G_{hh}\, \hat{T}(\overline{w}), \\ \hat{\hat{v}}_i &= G_{ih}\, \hat{T}(\overline{w}). \end{aligned} \tag{21}$$

At this stage it is important to emphasize the fact that the whole matrix G need not be calculated. As shown above, only the first column is necessary to obtain both T and the response of the rest of the flexible link. A lot of computational effort may be saved by this fact, since once the matrix **H** has been triangularized only one forward reduction and backsubstitution have to be performed to calculate the first column of **G.**

The final results in the time domain may be obtained through the application of the inverse fast Fourier transform.

APPLICATION

The formulation explained above is applied to a flexible link like that shown in Figure 1, with the following characteristics:

length = 150 cm,
damping ratio = 0.02,
$E = 2 \times 10^7$ N/cm^2,
$\rho = 0.008$ kg/cm^3,
$I = 0.25 \times 10^{-2}$ cm^4,
$A = 1$ cm^2,
$I_H = 1000$ kg $\times$ cm^2.

The link is divided into 10 finite elements, giving a total of 21 degrees of freedom. The first element is considered 10 times more rigid than the rest to account for the stiffness of the hub.

The imposed tip acceleration and displacement are shown in Figures 3 and 4, respectively. After the finite element consistent mass and stiffness matrices are formed, a modal analysis gives the following first periods of vibration:

$T_0 = \infty$ (rigid body motion),
$T_2 = 0.525$ sec,
$T_2 = 0.182$ sec,
$T_3 = 0.0732$ sec,
$T_4 = 0.0375$ sec,
$T_5 = 0.0220$ sec.

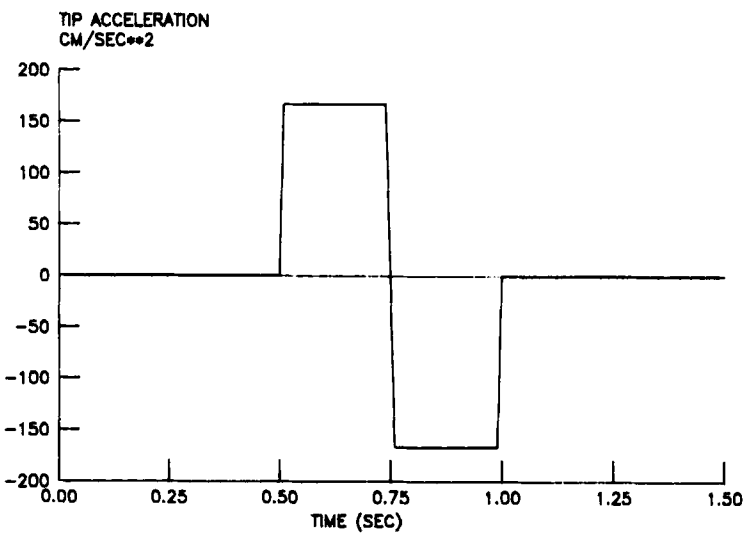

Figure 3. Imposed tip acceleration.

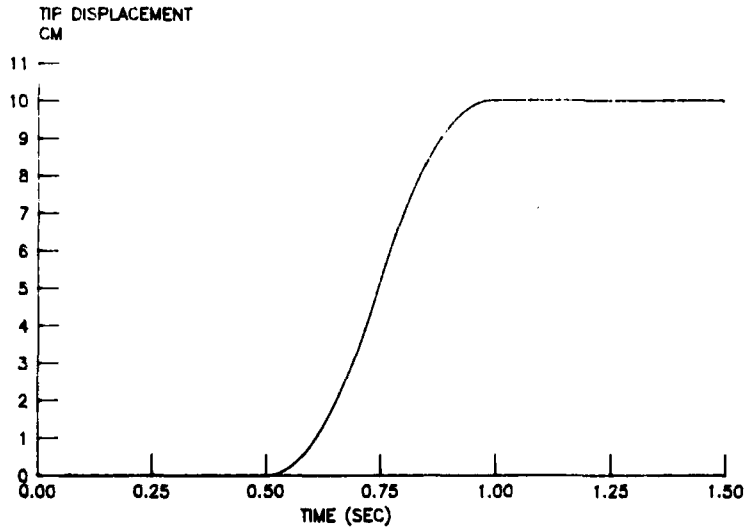

Figure 4. Imposed tip displacement.

The torque that needs to be applied at the hub to produce the desired tip motion is calculated according to the procedure explained above, and it is shown in Figure 5. This figure also illustrates the torque needed to produce the same tip motion on an infinitely rigid link having the same mass as that of the flexible link. The peak value of the torque for the flexible link is half of that required in the rigid link. It is worth

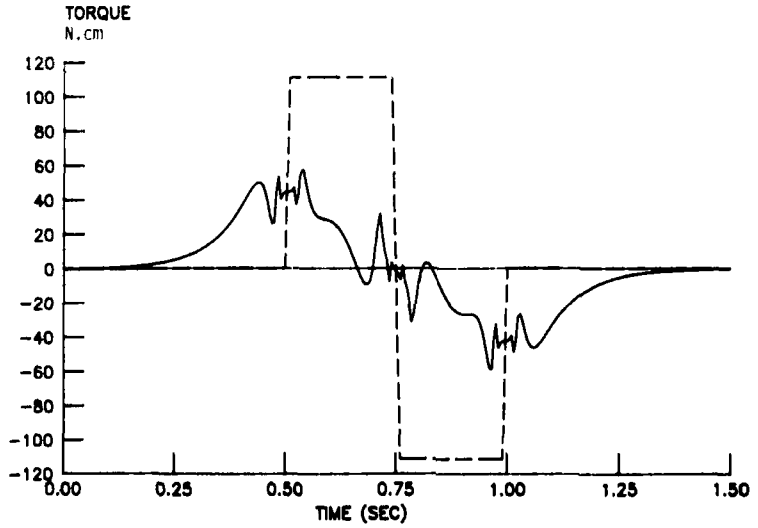

Figure 5. Calculated torques for the flexible link $I = \frac{1}{4}\ 10^{-2}\ cm^4$ (solid line) and the rigid link (dashed line).

pointing out that when a direct dynamic analysis is performed and the system is analyzed with the calculated torque as input, tip displacement, and accelerations are obtained which exactly coincide with the desired ones.

These results also show that in order to get the imposed tip motion of the flexible link the torque needs to be applied 0.3 sec before the actual tip displacement starts taking place. This is due to the fact that waves along the link move at a finite speed that depends on the arm flexibility and frequency of excitation. This finite wave speed introduces a time lag between actuator and tip response. The torque keeps on actuating another 0.3 sec after the tip has reached its final position, during this time the torque is absorbing or compensating the reflected waves that come from the tip. Figure 6 compares the hub rotation of the flexible link to that of the rigid link.

A second example is run with the same link, but with its moment of inertia modified to $I = 10^{-2}$ cm^4; that is, four times more rigid than the previous one. This configuration may be considered more rigid than flexible. The torque needed to produce the desired motion in this case is plotted against that needed in the case of an infinitely rigid link in Figure 7. As can be seen, the calculated torque is more equal to the rigid link torque; furthermore, the time lag between actuating time and response is smaller than in the previous case. This is because of the increase of wave velocity due to the corresponding increase of rigidity.

Figures 8 and 9 show the oscillations of the tip motion when the torque that produces the desired tip motion in a rigid link is applied to the flexible links of inertia $I = \frac{1}{4}$ 10^{-2} cm^4 and $I = 10^{-2}$ cm^4, respectively. The tip reaches the desired end position only after several seconds in which the tip oscillates near that position. Figures 8 and 9 also show how after 4.5 sec the tip is still oscillating heavily in the case of $I = \frac{1}{4}$

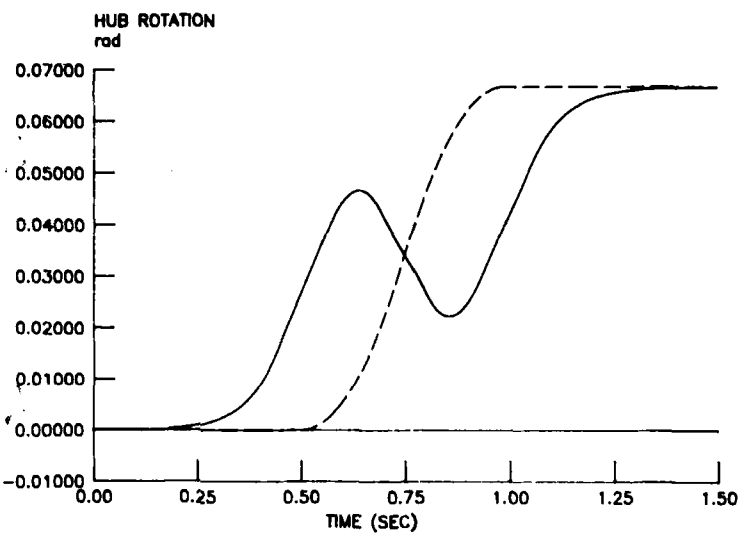

Figure 6. Rotations at the hub. Flexible link $I = \frac{1}{4}$ 10^{-2} cm^4 (solid line) and rigid link (dashed line).

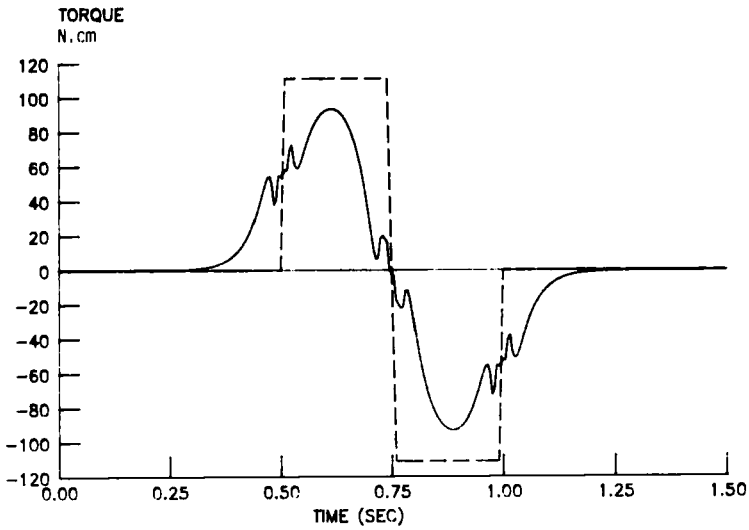

Figure 7. Calculated torques for the flexible link $I = 10^{-2}$ cm^4 (solid line) and the rigid link (dashed line).

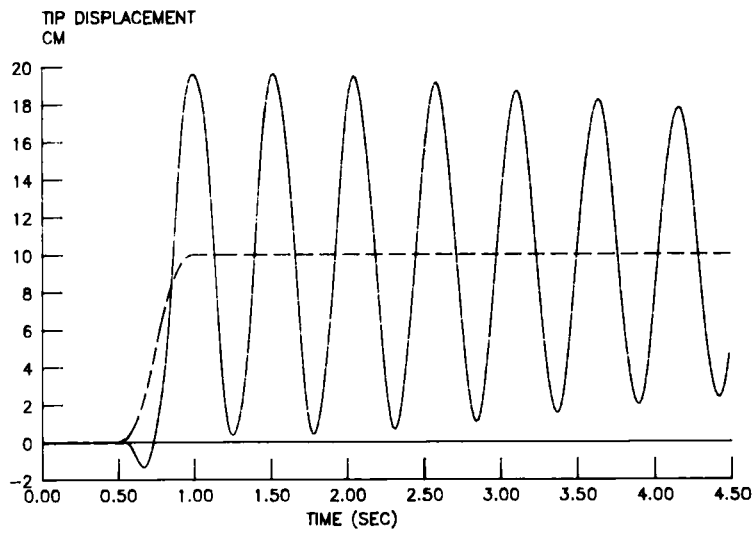

Figure 8. Tip displacements produced by rigid-link torque in the flexible link $I = \frac{1}{4}\ 10^{-2}$ cm^4 (solid line) and in the rigid link (dashed line).

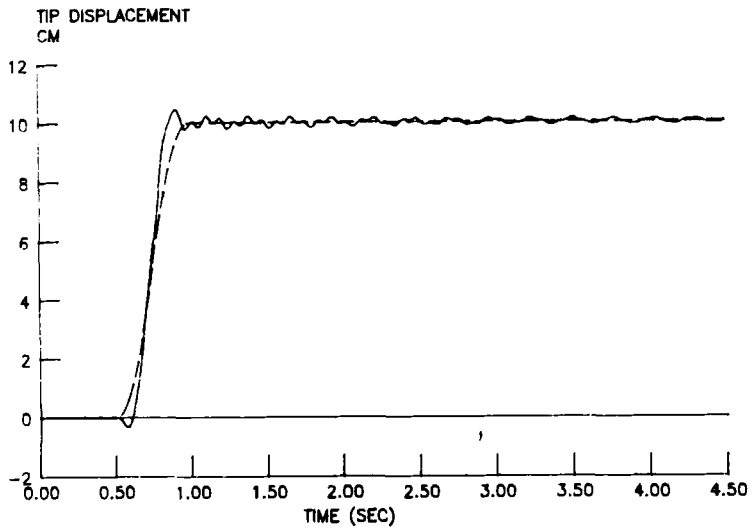

Figure 9. Tip displacements produced by rigid-link torque in the flexible link $I = 10^{-2}$ cm^4 (solid line) and in the rigid link (dashed line).

10^{-2} cm^4 and slightly for $I = 10^{-2}$ cm^4. This waiting time is much larger than that needed for the computed torque to compensate the reflecting waves in the flexible links.

CONCLUSIONS

A method has been presented for the calculation of the end torque that is required to produce a desired motion at the tip of a flexible link. This method is based on a finite-element frequency-domain formulation for the solution of the equations of motions that define the flexible behavior of the link. The computed torque, which is much smaller than that required for a rigid link of the same weight, reproduces exactly the desired tip motion without overshoot. The implicit assumption of a linear response in the system is necessary for the frequency domain analysis to be applicable.

The expansion of the desired end motion into its harmonic components helps to understand the wave-propagation nature of the problem, by which the different waves generated by the torque at one end propagate along the link and subsequently reflect back at the other end to return to their original position. The applied example demonstrates the accuracy of the method.

The proposed technique is suitable for open-loop control, and it may provide a good closed-loop control law. Further work is necessary to increase the numerical efficiency of the method and to extend it to multilink robots. These are the subjects of future work that the author will undertake.

The author would like to acknowledge the support of this work by the National Science Foundation, Grant No. 8421415, through the Center for Robotics Systems in Microelectronics.

References

1. W. H. Sunada and S. Dubowsky, "On the Dynamic Analysis and Behaviour of Industrial Robotic Manipulators with Elastic Members," *ASME J. Mechan. Transmiss. Autom. Design*, **105**, 42–50 (1983).
2. L. W. Chang, "Dynamic Analysis of Robotic Manipulators with Flexible Links," Ph.D. thesis, Purdue University, 1984.
3. M. Geradin, G. Robert, and G. Bernardin, "Dynamic Modelling of Manipulators with Flexible Members," in: *Advanced Software in Robotics*, A. Dantline and M. Geradin (Eds.), Elsevier, North-Holland, 1984, pp. 27–39.
4. G. Naganathan and A. H. Soni, "Non-Linear Flexibility Studies for Spatial Manipulators," in: *Proceedings of the 1986 IEEE International Conference on Robotics and Automation, San Francisco, April 1986*, pp. 373–378.
5. R. Cannon and E. Schmitz, "Initial Experiments on End-Point Control of a Flexible One-Link Robot," *Int. J. Robotics Res.* **3**,(3), 62–75 (1984).
6. I. Sakawa, F. Matsuno, and S. Fukushima, "Modelling and Feedback Control of a Flexible Arm," *J. Robotic Syst.*, **2**, 453–472 (1985).
7. P. Karkkainen, "Compensation Manipulator Flexibility Effects by Modal Space Techniques," in: *Proceedings of the 1985 IEEE International Conference on Robotics and Automation, St. Louis, March 1985*, pp. 972–977.
8. A. G. Chassiakos and G. A. Bekey, "Pointwise Control of a Flexible Manipulator Arm," in: *SYROCO '85. Barcelona, November 1985*, pp. 113–117.
9. S. Nicosia, P. Tomei, and A. Tornambe, "Dynamic Modelling of Flexible Robot Manipulators," in: *Proceedings of the 1986 IEEE International Conference on Robotics and Automation, San Francisco, April 1986*, pp. 365–372.
10. K. J. Bathe, *Finite Element Procedures in Engineering Analysis*, Prentice-Hall, Englewood Cliffs, NJ, 1982, Chap. 5.
11. T. K. Caughey, "Classical Normal Modes in Damped Linear Systems," *J. Appl. Mechan.*, **27**, 269–271 (1960).
12. L. Meirovitch, *Analytical Methods in Vibrations*, Macmillan, New York, 1967, Chap. 9.